Neurosciences

International Edition: DOI: 10.1002/anie.201409597
German Edition: DOI: 10.1002/ange.201409597

Selective Aptamer-Based Control of Intraneuronal Signaling**

*Sabine Lennarz, Therese Christine Alich, Tony Kelly, Michael Blind, Heinz Beck, and Günter Mayer**

Abstract: *Cellular behavior is orchestrated by the complex interactions of a myriad of intracellular signal transduction pathways. To understand and investigate the role of individual components in such signaling networks, the availability of specific inhibitors is of paramount importance. We report the generation and validation of a novel variant of an RNA aptamer that selectively inhibits the mitogen-activated kinase pathway in neurons. We demonstrate that the aptamer retains function under intracellular conditions and that application of the aptamer through the patch-clamp pipette efficiently inhibits mitogen-activated kinase-dependent synaptic plasticity. This approach introduces synthetic aptamers as generic tools, readily applicable to inhibit different components of intraneuronal signaling networks with utmost specificity.*

The investigation of intracellular signaling has moved from the discovery of the first intracellular signaling molecule to the appreciation of intracellular signaling as a complex and highly organized network in which thousands of molecular partners interact.[1] Unraveling such multidimensional interactions requires inhibitors that potently and specifically block individual components of signaling cascades. The strategy to develop such inhibitors has mainly focused on the generation of low-molecular-weight compounds. Developing such inhibitors is laborious and expensive, and requires sophisticated laboratories (e.g., organic chemical synthesis and high-throughput screening facilities with access to a comprehensive compound library). Without extensive optimization procedures many of these inhibitors have been found to display limited specificity and potency.[2] The development and maturation of initial lead compounds to enhance specificity and potency is also time-consuming and in many cases inefficient. Clearly, this traditional strategy of inhibitor development is slow, and has not kept pace with the rapid increase in knowledge about the components of intracellular signaling. This is particularly irksome because the advances in systems biology and application to diseases are yielding numerous hypotheses about disease mechanisms, which could be directly tested with specific inhibitors.[3]

Thus, there is an urgent need for a compound class that can be rapidly developed and is both specific and potent. Aptamers fulfil these criteria, but to date only a few examples have reported intracellular activity of aptamers.[4] This might be due to the high structural demands of aptamers, which require an intact 3D shape for target recognition and inhibition. For instance, aptamer folding is often affected by ion composition, which can disrupt binding under certain conditions.[5] However, herein we demonstrate that this can be overcome by appropriate reselection strategies. We developed an aptamer, named C5, which binds and inhibits the Mitogen-activated protein kinase (MAPK) Erk1/2 and remains functional under various conditions. The aptamer recognizes Erk1/2 in an ATP-competitive manner and is remarkably specific. C5 remains functional under various ionic conditions, qualifying it for intracellular applications. Although aptamers are of polyanionic nature, and therefore cannot pass cell membranes autonomously, we show that intracellular delivery of aptamers is easily accomplished using patch-clamp techniques. This approach does not require elaborate delivery strategies, for example, plasmid-based expression systems, and is thus broadly applicable.

Erk2 is a component of the mitogen-activated protein kinase (MAPK) pathway, which plays a central role in the regulation of many cellular functions.[6] In the central nervous system (CNS), Erk1/2 are essential for different forms of synaptic long-term plasticity,[7] which is referred to as the molecular mechanism proposed to underlie learning and memory. Aberrant Erk1/2 activity is also thought to contribute importantly to CNS disorders, such as epilepsy,[8] Alzheimer's disease,[9] stroke,[10] and cancer.[11] In all these disorders, the availability of selective and potent Erk1/2 inhibitors will be indispensable for the functional investigation of the individual role of Erk1/2 in neuronal signaling in both, the normal and diseased CNS. By combining patch-clamp electrophysiology with aptamer delivery, we demonstrate that C5 selectively inhibits a form of synaptic plasticity, termed spike-timing dependent plasticity (STDP) in neurons that requires MAPK activity, whereas MAPK-independent STDP was unaffected.

[*] Dr. S. Lennarz, Dr. M. Blind, Prof. Dr. G. Mayer
Life and Medical Sciences Institute, University of Bonn
Gerhard-Domagk-Str. 1, Bonn (Germany)
E-mail: gmayer@uni-bonn.de
MSc T. C. Alich, Dr. T. Kelly, Prof. Dr. H. Beck
Laboratory of Experimental Epileptology and Cognition Research
Department of Epileptology
Sigmund-Freud Str. 25, Bonn (Germany)
Prof. Dr. H. Beck
Deutsches Zentrum für Neurodegenerative Erkrankungen in der Helmholtz Gemeinschaft

[**] We thank Melanie Cobb (UT Southwestern, Texas) for kindly providing expression vectors for Erk1,[18] S. Knapp (Structural Genomics Consortium, University of Oxford (UK)) for providing kinases, and V. Fieberg for technical assistance regarding protein purification. Financial support by the NRW LIMES Graduate School Chemical Biology (to S.L.) and by the DFG SFB1089 (to H.B. and G.M.) and the DIP grant Zi 1172/2-1 (to H.B.) is acknowledged. G.M. acknowledges also support from the European Research Council under the European Union's Seventh Framework program (FP7/2007-2013)/ERC Grant agreement no. 615381 (acronym: OptoRibo).

Supporting information for this article is available on the WWW under http://dx.doi.org/10.1002/anie.201409597.

Intracellular use of aptamers in neurons requires maintained aptamer activity in the intracellular milieu. We found that the known Erk1/2-binding aptamer TRA[12] is susceptible to variations of ionic composition (Figure S1 in the Supporting Information, SI). We therefore sought to identify an aptamer variant that shares the Erk1/2-inhibiting properties of TRA but is less susceptible to variations in ionic composition. We synthesized a TRA-based nucleic acid library, comprising a partially randomized region (Figure S1a). This RNA library was subjected to an in vitro selection procedure targeting active Erk2 (pp-Erk2) under more physiologically relevant conditions, which we have applied previously to successfully identify aptamers that retain activity in the intracellular milieu.[4a,b,13] After six selection cycles, cloning and sequencing revealed two sequences, namely C1 and C5 (Figures 1a and S2). Compared to the

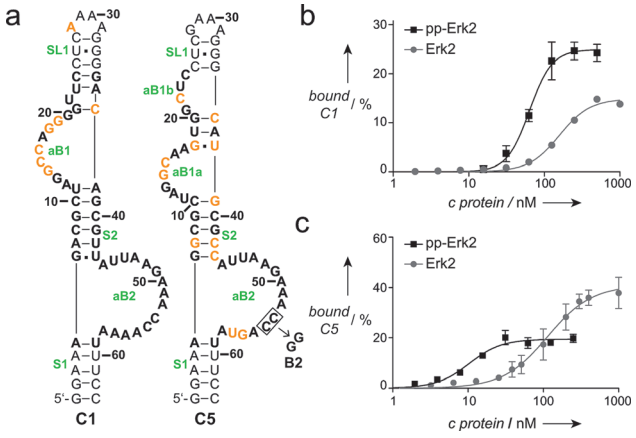

Figure 1. The RNA aptamer C5 interacts with Erk2. a) Putative secondary structure of the aptamers C1 and C5 yielded by reselection using a doped TRA-library (see also Figure S1a). Nucleotides initially randomized are depicted in bold letters. Nucleotides that differ from the original aptamer are highlighted in orange. Two point mutations (named B2) at the indicated (boxed) position led to a significant reduction of C5's ability to interact with Erk2 (see also Figure S4a). Determination of the K_D-values of C1 (b) and C5 (c) binding to active Erk2 (pp-Erk2) or inactive Erk2 (see also Table 1). The amount of radioactively labeled RNA is plotted against the protein concentration. All experiments were performed at least twice (mean ± SEM).

original aptamer, C1 has seven mutations whereas C5 bears twelve. Most of the mutations are located either in the asymmetric bulge aB1 (aptamer C1 and C5) or the central stem S2 (aptamer C5; Figure 1a). In contrast, the asymmetric bulge aB2 is not mutated in aptamer C1. C5 has only two mutations in this region. This indicates that aB2 is highly conserved. In C5, nucleotide G35 of the stem loop SL1 is deleted, whereas C1 bears one mutation, namely A37C, in this domain.

Filter retention analysis revealed binding of C1 and C5 to active Erk2 with an affinity of ca. 63 nM and 10 nM, respectively, and recognition of inactive Erk2 with a 2.5- and 10-fold lower affinity (K_D-values ≈ 158 nM for C1 and ≈ 114 nM for C5; Table 1, Figure 1b,c). Moreover, interaction of C5 with Erk2 was tolerant to a variety of ionic conditions (Figure S3, Table S1). Based on these data we decided to

Table 1: K_D-values of C1 and C5 for different MAP kinases.[a]

MAP kinase	C1 K_D[b]	C5 K_D[b]
pp-Erk2	63.6 ± 4.5	10.3 ± 1.1
Erk2	158.5 ± 8.5	113.7 ± 26.1
Erk1	not determined	94.1 ± 9.5
P38α	not determined	not detectable
JNK2α	not determined	not detectable

[a] K_D-values were determined as described in material and methods. All experiments were performed at least twice. pp-Erk2: active Erk2.
[b] Values given in [nM].

focus on C5 for further characterization. As non-binding control sequences, we included either a scrambled version of C5 (C5sc) or a double-point mutant, termed B2 (Figure 1a, right panel; Figure S4a).

We next investigated the specificity of C5. As summarized in Table 1, C5 recognizes inactive Erk1 with a similar affinity (K_D-value ≈ 94 nM) as found for inactive Erk2. Most notably, we did not detect any binding to the related MAP kinases p38α or JNK2α (Figure 2a). We then extended the analysis to a panel of ten kinases from different subfamilies.[14] At a concentration of 1 μM, which is 10-fold above its observed K_D for inactive Erk2 and even 100-fold above the K_D for active Erk2, C5 did not interact with any of the kinases investigated (Figure 2b), indicating an exceptional specificity for Erk1/2. To investigate whether C5 also interacts with endogenous Erk1/2, we performed aptamer pull-down assays employing biotinylated C5 immobilized on streptavidin-coated magnetic beads. These beads were incubated with cell lysates. After washing, the remaining components were eluted and investigated by immunoblot analysis. These experiments demonstrated that C5 also interacts with endogenous Erk1/2 (Figure 2c). Taken together, our studies establish C5 as an aptamer with high affinity and specificity for Erk1/2.

We next performed competition experiments, in which binding of radioactively labeled C5 to Erk2 was monitored in the presence of increasing amounts of ATP or UTP. ATP was found to compete with C5 for Erk2 binding and an IC_{50}-value of ca. 1 mM was determined (Figure 3a, grey circles). Noteworthy, this value is in the same range as the reported K_D-value of Erk2 for ATP.[15] Addition of UTP at concentrations up to 2 mM had no effect on aptamer binding (Figure 3a, black squares), whereas at higher concentrations competition was observed that most likely is due to unspecific interactions of UTP with the RNA aptamer, for example, by base pairing.

In line with this finding, C5 also inhibits Erk2 kinase activity (Figure 3b). Co-incubating active Erk2 with the substrate Elk1 and increasing concentrations of C5 showed this. As a measure of Erk2 activity, transfer of γ-^{32}P from ATP to Elk1 was determined. C5 inhibits Erk2 in a concentration-dependent manner, whereas the B2 control RNA has no effect (Figure 3b). Since C5 does not interact with Elk1 under the conditions employed in the kinase assay (Figure S4b), inhibition of Elk1-phosphorylation is likely attributed to direct inhibition of Erk2 by C5.

Having established C5 as a potent and highly selective Erk1/2 inhibitor we ultimately tested if C5 is also capable of

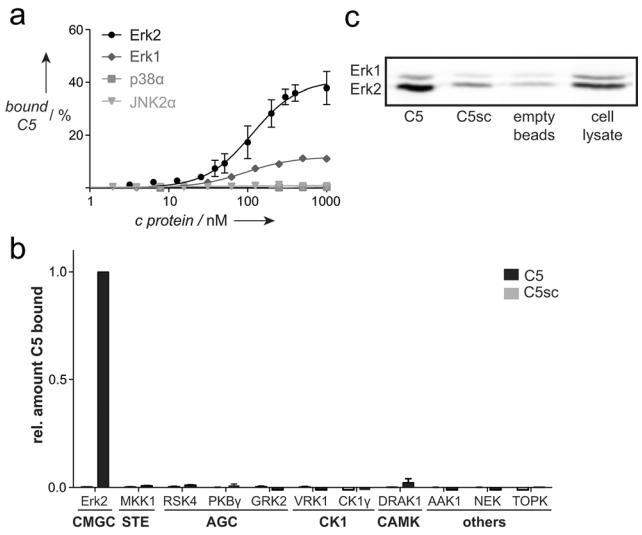

Figure 2. Interaction analysis of C5. a) K_D-value determination of C5 binding to different MAP kinases. The amount of radioactively labeled RNA is plotted against the protein concentration. All experiments were performed at least twice (mean ± SEM). C5 binds to Erk2 (note that the black curve is the same curve as the grey curve shown in Figure 1c) and Erk1. No binding to p38α or JNK2α could be detected. b) Specificity analysis. The amount of bound radioactively labeled C5 or control RNA (C5sc) was normalized onto the amount of radioactively labeled C5 bound to Erk2. C5 does not bind to kinases belonging to different subfamilies at a concentration of 1 μM ($n = 2$, mean ± SEM). Erk2: extracellular signal-regulated kinase 2, MEK1: Mitogen-activated protein kinase kinase 1, RSK4: 90 kDa ribosomal S6 kinase 4, PKBγ: protein kinase B γ, GRK2: G protein-coupled receptor kinase 2, VRK1: Vaccina-related kinase 1, CK1: casein kinase 1, DRAK1: DAP kinase-related apoptosis-inducing protein kinase 1, AAK1: AP2 associated protein kinase 1, NEK1: NimA related kinase 1, TOPK: Lymphokine-activated killer T-cell-originated protein kinase. c) Pull-down assay of endogenous Erk1/2. Specifically bound Erk1/2 was detected by SDS-PAGE and immunoblot analysis using an Erk1/2-specific antibody. Cell lysate was used as antibody and loading control. This assay shows that C5 interacts with endogenous Erk1/2. The blot shown is a representative example from three independent experiments.

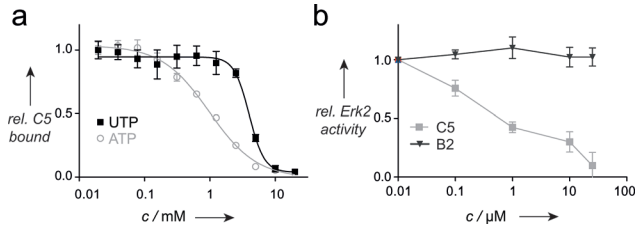

Figure 3. a) Competition of C5-binding to Erk2 by increasing concentrations of ATP or UTP. The amount of radioactively labeled C5 bound to Erk2 in the absence of NTPs was set to 1 ($n = 4$, mean ± SEM). b) Concentration-dependent inhibition of Erk2 activity by C5 (grey line) or B2 (black line) as monitored by phosphate incorporation into the substrate protein Elk-1. Erk2 activity was normalized onto samples without RNA ($n = 3$, mean ± SEM).

inhibiting Erk1/2-dependent intraneuronal signaling. It is well-established that synaptic activity leads to Ca^{2+} influx into neuronal dendrites, which then activates downstream signaling cascades, amongst them MAPK cascades. These then lead to modifications in ion channels and receptors, which mediate synaptic plasticity and a lasting enhancement in synaptic transmission (Figure 4a). In particular, hippocampal synaptic plasticity induced by coincident activation of synaptic inputs with postsynaptic action potentials leads to a lasting potentiation of synaptic transmission.[16] This form of plasticity is

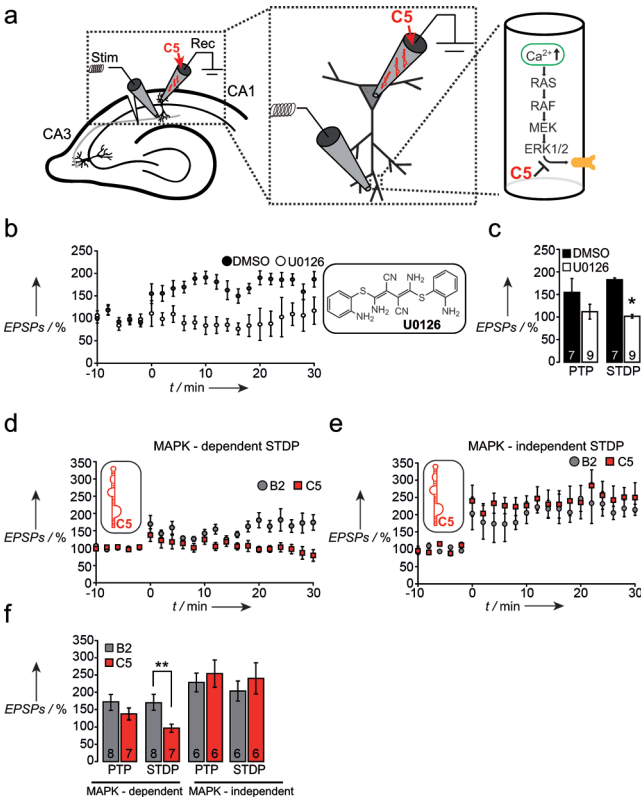

Figure 4. Aptamer-based inhibition of spike-timing LTP. a) Schematic of the recording configuration. Leftmost diagram shows a schematic of a hippocampal slice preparation, with the positioning of the stimulation (stim) and recording (rec) electrodes at a CA1 neuron. The first enlarged inset shows the patch-clamp electrode that provides access to the cell interior and through which the aptamers were delivered. The extracellularly located stimulation electrode is also depicted. The rightmost inset shows a schematic of a dendritic segment and the signaling cascade that affects ion channels and receptors (orange), which underlie STDP expression. b,c) Inhibition of STDP with the MEK inhibitor UO126 [40 μM]. STDP was induced with the pairing protocol shown in Figure S7a (MAPK-dependent STDP). STDP was induced with the pairing protocol shown in Figure S7a (MAPK-dependent STDP) at time point 0. We verified that this stimulation protocol indeed results in MAPK-dependent STDP by applying the inhibitor UO126 (40 μM in 0.4% DMSO, control recordings with DMSO only). Indeed, UO126 significantly inhibited the STDP induced with this protocol. Time course in panel (b), summary in panel (c). Asterisks indicate $p = 0.013$, Wilcoxon Rank test. N-numbers given within the bars. d,e) Average time course of experiments with C5 [1 μM] and the control B2 [1 μM] for MAPK-dependent STDP (panel d) and MAPK-independent STDP (panel e). f) Summary of the magnitude of the potentiation measured immediately after STDP induction (post-tetanic potentiation, PTP) and the magnitude of stable STDP (see Methods in the SI). The C5 aptamer selectively inhibited MAPK-dependent STDP. N-numbers given within the bars. Asterisks indicate significance, $p = 0.005$ Wilcoxon Rank test.

termed spike-timing dependent plasticity (STDP). Depending on the induction protocol, some forms of STDP require Erk1/2 activation, while others do not.[7c] To test how aptamer-based inhibition of Erk1/2 affects STDP, we obtained whole-cell patch-clamp recordings from CA1 neurons in acute hippocampal slice preparations obtained from mice (see the Methods Section in the SI, Figure 4a). We chose to use the patch-clamp approach for two main reasons. Firstly, because whole-cell patch-clamp recordings entail formation of a connection between the solution filling the patch pipette, and the intracellular space, this affords an excellent, albeit not yet realized option to introduce aptamers into cells. Advantageously, this method does not require cloning and expression of the aptamer from genes introduced in cells. Even more importantly, this approach allows measuring the electrical response of the cell. It thus allows assessing the functional outcome of a very precise manipulation of intracellular signal transduction. Here, we demonstrated that indeed the patch-clamp technique allows the introduction of either C5 or the control RNA B2 into CA1 neurons under conditions that retain the aptamers' interaction properties and integrity (Figure S5). Neither C5 nor the B2 control RNA altered the passive or active functional properties of CA1 neurons (Figure S6). Excitatory postsynaptic potentials (EPSPs) were evoked by Schaffer collateral stimulation (Figure 4a), and were adjusted to about 2 mV (B2: 1.8 ± 0.3; C5: 1.8 ± 0.2). Subsequently, STDP was induced using two different protocols. In both protocols, repeated burst stimulation was applied with a single burst consisting of 5 stimuli at 100 Hz (see the Methods Section in the SI for details). In the first variation of this protocol, only two intraburst stimuli were paired with postsynaptic action potentials (Figure S7a). In the second variation of this protocol, each Schaffer collateral EPSP was paired with a postsynaptic action potential (Figure S7b). As described previously, the MEK inhibitor UO126 blocks STDP induced by the first stimulation protocol (Figure 4b,c). This confirms that the first variation of this stimulus protocol is dependent on the MAPK pathway.

We then evaluated if inhibiting Erk1/2 by C5 also affects MAPK-dependent STDP (Figure 4d,f). Induction of MAPK-sensitive STDP was unaffected by the B2 control RNA, whereas potentiation was blocked by C5 (Figure 4d,f). In contrast, MAPK-independent STDP was indistinguishable between neurons treated with B2 or C5 (Figure 4e,f). These results indicate that selective inhibition of Erk1/2 in neurons by C5 results in a specific ablation of MAPK-dependent forms of plasticity. One potential contaminating factor in such experiments is that baseline transmission might be reduced by C5 or B2, reducing the excitation during STDP induction, and consequently the amount of STDP expressed. However, effects on the properties of spikes generated during the LTP induction protocol did not differ between the B2 and C5 groups (Figure S8a). Likewise, perfusion of aptamers caused no differences in the properties of baseline Schaffer collateral EPSPs (Figure S8b,c).

In summary, we demonstrate that aptamers are a true alternative to commonly used low molecular weight inhibitors for dissecting intracellular signaling in neurons. The approach as described here has several key advantages. First, the combination of aptamers and electrophysiology is of course not limited to the aptamer used herein but rather can be applied to many other aptamer–target pairs. Importantly, the selection process can be automated,[17] allowing generation of aptamers for hundreds of target proteins within a reasonable time frame and with manageable costs. Second, our approach provides aptamers through the patch-clamp pipette. In the field of single-cell analysis and neuroscience, this is a particularly compelling approach. For example, virtually all signaling within the CNS is subserved by synaptic communication between neurons. The patch-clamp technique therefore allows combining aptamer-mediated inhibition of signal transduction with a precise analysis of key functional cellular properties, for example, impact of MAP kinase signaling on ion-channel function as shown in this study. A further advantage of the patch-clamp approach is that it obviates laborious expression approaches of aptamers, which are not applicable in a high-throughput manner in native cells. Rather, it can be readily applied to a plethora of different neuronal types present in the brain, as long as they are accessible to patch-clamp recordings. That these techniques can be applied to native neurons in ex vivo preparations is very important, because immortalized cell lines or primary cell cultures have fundamentally different functional properties when compared to native neurons. The ready availability of both aptamers and patch-clamp technology will enable the use of aptamers by a broad scientific community, in native neurons and other single-cell experiments. A key advantage of this approach is the rapid transformation of aptamers identified in the test tube into intracellular inhibitors. The simplicity and rapidity of implementation has in our opinion tremendous potential to fuel rapid confirmatory strategies in systems chemistry and biology.

Keywords: aptamers · MAP kinase · neurosciences · SELEX

How to cite: *Angew. Chem. Int. Ed.* **2015**, *54*, 5369–5373
Angew. Chem. **2015**, *127*, 5459–5463

[1] T. Hunter, *Cell* **2000**, *100*, 113–127.
[2] U. Rix, L. L. Remsing Rix, A. S. Terker, N. V. Fernbach, O. Hantschel, M. Planyavsky, F. P. Breitwieser, H. Herrmann, J. Colinge, K. L. Bennett, M. Augustin, J. H. Till, M. C. Heinrich, P. Valent, G. Superti-Furga, *Leukemia* **2010**, *24*, 44–50.
[3] K. A. Fujita, M. Ostaszewski, Y. Matsuoka, S. Ghosh, E. Glaab, C. Trefois, I. Crespo, T. M. Perumal, W. Jurkowski, P. M. A. Antony, N. Diederich, M. Buttini, A. Kodama, V. P. Satagopam, S. Eifes, A. Del Sol, R. Schneider, H. Kitano, R. Balling, *Mol. Neurobiol.* **2014**, *49*, 88.
[4] a) L. L. Lebruska, L. J. Maher, 3rd, *Biochemistry* **1999**, *38*, 3168–3174; b) G. Mayer, M. Blind, W. Nagel, T. Böhm, T. Knorr, C. L. Jackson, W. Kolanus, M. Famulok, *Proc. Natl. Acad. Sci. USA* **2001**, *98*, 4961–4965; c) M. G. Theis, A. Knorre, B. Kellersch, J. Moelleken, F. Wieland, W. Kolanus, M. Famulok, *Proc. Natl. Acad. Sci. USA* **2004**, *101*, 11221–11226; d) M. J. Lange, T. K. Sharma, A. S. Whatley, L. A. Landon, M. A. Tempesta, M. C. Johnson, D. H. Burke, *Mol. Ther.* **2012**, *20*, 2304–2314; e) H. Kwak, I. Hwang, J. H. Kim, M. Y. Kim, J. S. Yang, S. Jeong, *Mol. Cancer Ther.* **2009**, *8*, 2664–2673; f) H. K. Lee, H. Y. Kwak, J. Hur, I. A. Kim, J. S. Yang, M. W. Park, J. Yu, S. Jeong, *Cancer Res.* **2007**, *67*, 9315–9321.

[5] a) L. A. Cassiday, L. J. Maher, 3rd, *Biochemistry* **2001**, *40*, 2433 – 2438; b) R. L. Strack, M. D. Disney, S. R. Jaffrey, *Nat. Methods* **2013**, *10*, 1219 – 1224; c) J. M. Tome, A. Ozer, J. M. Pagano, D. Gheba, G. P. Schroth, J. T. Lis, *Nat. Methods* **2014**, *11*, 683 – 688.
[6] a) G. Pearson, F. Robinson, T. Beers Gibson, B. E. Xu, M. Karandikar, K. Berman, M. H. Cobb, *Endocr. Rev.* **2001**, *22*, 153 – 183; b) R. Roskoski, Jr., *Pharmacol. Res.* **2012**, *66*, 105 – 143.
[7] a) J. A. Rosenkranz, A. Frick, D. Johnston, *J. Physiol.* **2009**, *587*, 115 – 125; b) J. D. Sweatt, *Curr. Opin. Neurobiol.* **2004**, *14*, 311 – 317; c) G. M. Thomas, R. L. Huganir, *Nat. Rev. Neurosci.* **2004**, *5*, 173 – 183.
[8] C. Bernard, A. Anderson, A. Becker, N. P. Poolos, H. Beck, D. Johnston, *Science* **2004**, *305*, 532 – 535.
[9] H.-W. Klafki, P. Lewczuk, H. Kamrowski-Kruck, J. M. Maler, K. Müller, O. Peters, I. Heuser, F. Jessen, J. Popp, L. Frölich, S. Wolf, B. Prinz, C. Luckhaus, J. Schröder, J. Pantel, H.-J. Gertz, H. Kölsch, B. W. Müller, H. Esselmann, M. Bibl, J. Kornhuber, J. Wiltfang, *J. Alzheimer's Dis.* **2009**, *18*, 613 – 622.
[10] K. Szydlowska, A. Gozdz, M. Dabrowski, M. Zawadzka, B. Kaminska, *J. Neurochem.* **2010**, *113*, 904 – 918.
[11] D. Chen, D. Zuo, C. Luan, M. Liu, M. Na, L. Ran, Y. Sun, A. Persson, E. Englund, L. G. Salford, E. Renström, X. Fan, E. Zhang, *PLoS ONE* **2014**, *9*, e87281.
[12] S. D. Seiwert, T. Stines Nahreini, S. Aigner, N. G. Ahn, O. C. Uhlenbeck, *Chem. Biol.* **2000**, *7*, 833 – 843.
[13] a) H. Shi, B. E. Hoffman, J. T. Lis, *Proc. Natl. Acad. Sci. USA* **1999**, *96*, 10033 – 10038; b) H. H. Salamanca, N. Fuda, H. Shi, J. T. Lis, *Nucleic Acids Res.* **2011**, *39*, 6729 – 6740.
[14] G. Manning, D. B. Whyte, R. Martinez, T. Hunter, S. Sudarsanam, *Science* **2002**, *298*, 1912 – 1934.
[15] a) C. N. Prowse, J. C. Hagopian, M. H. Cobb, N. G. Ahn, J. Lew, *Biochemistry* **2000**, *39*, 6258 – 6266; Erratum C. N. Prowse, J. C. Hagopian, M. H. Cobb, N. G. Ahn, J. Lew, *Biochemistry* **2000**, *39*, 14002; b) C. N. Prowse, J. Lew, *J. Biol. Chem.* **2001**, *276*, 99 – 103.
[16] H. Markram, J. Lübke, M. Frotscher, B. Sakmann, *Science* **1997**, *275*, 213 – 215.
[17] J. C. Cox, A. Hayhurst, J. Hesselberth, T. S. Bayer, G. Georgiou, A. D. Ellington, *Nucleic Acids Res.* **2002**, *30*, e108.
[18] A. Khokhlatchev, S. Xu, J. English, P. Wu, E. Schaefer, M. H. Cobb, *J. Biol. Chem.* **1997**, *272*, 11057 – 11062.

Received: September 29, 2014
Revised: January 29, 2015
Published online: March 5, 2015

